A Molecular Hybrid for Mitochondria-Targeted NO Photodelivery

Federica Sodano+,[a] Elena Gazzano+,[b] Aurore Fraix,[c] Barbara Rolando,[a] Loretta Lazzarato,[a] Marina Russo,[c] Marco Blangetti,[a] Chiara Riganti,*[b] Roberta Fruttero,*[a] Alberto Gasco,[a] and Salvatore Sortino*[c]

The design, synthesis, spectroscopic and photochemical properties, and biological evaluation of a novel molecular hybrid that is able to deliver nitric oxide (NO) into mitochondria are reported. This molecular conjugate unites a tailored o-CF$_3$-p-nitroaniline chromophore, for photo-regulated NO release, and a rhodamine moiety, for mitochondria targeting, in the same molecular skeleton via an alkyl spacer. A combination of steady-state and time-resolved spectroscopic and photochemical experiments demonstrate that the two chromogenic units preserve their individual photophysical and photochemical properties in the conjugate quite well. Irradiation with violet light triggers NO release from the nitroaniline moiety and photoionization in the rhodamine center, which also retains considerable fluorescence efficiency. The molecular hybrid preferentially accumulates in the mitochondria of A549 lung adenocarcinoma cells where it induces toxicity at a concentration of 1 μM, exclusively upon irradiation. Comparative experiments, carried out with ad-hoc-synthesized model compounds, suggest that the phototoxicity observed at such a low concentration is probably not due to NO itself, but rather to the formation of the highly reactive peroxynitrite that is generated from the reaction of NO with the superoxide anion.

Introduction

The mitochondrion is a key organelle that exerts a variety of cellular functions, including the production of ATP, regulation of cellular energy, redox metabolism, and apoptosis. Cellular viability is strictly dependent on mitochondrial functionality. Mitochondria have recently been considered as an important target for new antitumor drug development.[1–3] Interestingly, cancer cells show peculiar mitochondrial dysfunctions that can be harnessed for selective toxicity, with respect to normal-transformed cells.[4,5] Nitric oxide (NO), a ubiquitous messenger which plays important roles in many physiological and pathological processes,[6,7] exerts profound effects on mitochondria. Within these organelles, it may either originate from a nitric oxide synthase (NOS) isoform, anchored to the cytosolic face of the outer mitochondrial membrane, or, possibly, from a mitochondrial NOS located inside mitochondria.[8,9] Low amounts of NO can modulate the mitochondrial electron transport chain and stimulate mitochondrial biogenesis. By contrast, high levels of NO induce toxicity, principally via inhibition of the tricarboxylic acid cycle and mitochondrial respiration following NO binding with the heme group in cytochrome c oxidase, by stimulating the production of an excess of reactive nitrogen (RNS) and oxygen (ROS) species from mitochondria, as well as by stimulating mitochondrial apoptosis.[8] In particular, a prolonged increase in the superoxide anion ($O_2^{•-}$), due to a continued interaction between NO and cytochrome c oxidase, gives rise to a decreased concentration of glutathione and to the formation of peroxynitrite ($ONOO^-$). This latter, in turn, produces hydroxyl ($OH^•$) and nitrogen dioxide ($NO_2^•$) radicals, two very toxic species.[9,10] Consequently the accumulation of appropriate NO donors (NODs), namely products able to release NO under physiological conditions,[11] inside mitochondria may well be an efficient strategy with which to develop new anticancer drugs. This accumulation can be achieved via the covalent joining of a NOD with an appropriate targeting unit that displays high affinity for this cellular compartment. The use of classical NODs for this approach suffers from a number of important limitations. Indeed, NO release from these precursors lacks concentration control, can require enzymatic activation, can give rise to byproducts that may have significant toxicity and can modify some physiological parameters (i.e., pH and ionic strength).[12] Light is a powerful tool for the introduction of NO into biological systems and can overcome the above drawbacks using suitable NO photodonors (NOPDs).[13] Indeed these light-activated precursors allow the action of NO

[a] Dr. F. Sodano,+ Prof. B. Rolando, Dr. L. Lazzarato, Dr. M. Blangetti, Prof. R. Fruttero, Prof. A. Gasco
Department of Science and Drug Technology, University of Torino, 10125 Torino (Italy)
E-mail: roberta.fruttero@unito.it

[b] Dr. E. Gazzano,+ Prof. C. Riganti
Department of Oncology, University of Torino, Via Santena 5/bis, 10126 Torino (Italy)
E-mail: chiara.riganti@unito.it

[c] Dr. A. Fraix, Dr. M. Russo, Prof. S. Sortino
Laboratory of Photochemistry, Department of Drug Sciences, University of Catania, 95125 Catania (Italy)
E-mail: ssortino@unict.it

[+] These authors contributed equally to this work.

Supporting information and the ORCID identification number(s) for the author(s) of this article can be found under:
https://doi.org/10.1002/cmdc.201700608.

to be confined within the irradiated area with high spatial precision and its dosage to be controlled with great accuracy by tuning the duration and intensity of the irradiation.[13] NOPDs must satisfy some conditions before being used for biological research studies. These conditions include excitation with visible light and the absence of the formation of either toxic or visible light absorbing side photoproducts. These conditions are fulfilled by simple *p*-nitroaniline derivatives that bear a CF₃ group in the *o*-position and that have been extensively developed in our group.[14] As with other sterically hindered nitro derivatives,[15] they release NO under the action of violet light following nitro-to-nitrite rearrangement, the cleavage of the O—NO bond, the generation of a phenoxy radical as a key intermediate and the final formation of a phenol derivative as a stable product. Non planar torsional conformation of the nitro group in relation to the aromatic ring facilitates the rearrangement.[14a, 15a] Prompted by our on-going interest in building light-controlled NO delivering hybrid drugs,[16–18] and considering the limited number of studies into mitochondria-targeted NO photodelivery,[19, 20] we herein report the design, synthesis, spectroscopic and photochemical characterization and the biological evaluation of molecular hybrid **7** (Scheme 1). It cova-
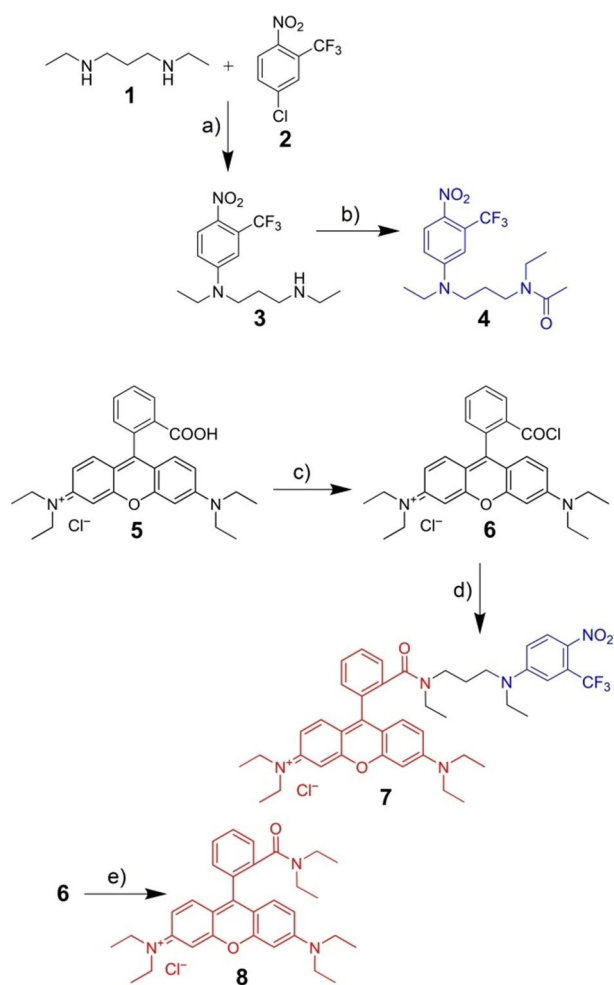
lently binds a suitable NOPD unit, *p*-nitroaniline derivative **3**, and rhodamine B **5**, a well-known mitochondrial probe,[21] within the same molecular skeleton via an amide bridge. The potential of hybrid **7** as an antitumor drug, following its accumulation into the mitochondria of human A549 lung adenocarcinoma cells, and its capacity to release NO under the action of violet light are discussed and compared with those of suitable model compounds **8**, which lack the NOPD framework, and **4**, which lacks the targeting unit.

Results and Discussion

Design and synthesis

The preservation of the photochemical properties of a photoresponsive molecule (i.e., NOPD), once it is covalently linked to another chromophoric unit to form a molecular hybrid, is not a trivial matter. Indeed, communication between the two chromophoric centers via unexpected photoinduced energy/electron transfer can be highly competitive with the desired photochemical process, precluding the final goal.[22] These interchromophoric interactions can be intentionally avoided with a careful choice of chromophoric groups that lack either spectral or redox complementarity.[22] Under these conditions, distinct photoresponsive centers can be operated in parallel even in close proximity, imposing multifunctional character to the resulting molecular hybrid. In particular, the possibility of exploiting the fluorescence of the targeting unit to image the hybrid while the photo-therapeutic unit releases its bioactive species permits imaging and therapy to be carried out in tandem and, therefore, can be especially valuable as a theranostic application. Conjugate **7** was devised with the above considerations in mind and its spectroscopic and photochemical properties confirm the validity of our design (see below).

   Products were prepared according to the pathways reported in Scheme 1. The direct coupling of commercial *N,N′*-diethylpropane-1,3-diamine **1** with 4-chloro-1-nitro-2-(trifluoromethyl)benzene **2** in acetonitrile at reflux gave rise to **3**, which, in turn, yielded the new NOPD **4**, when treated with acetic anhydride. The reaction of rhodamine **5** with POCl₃, in 1,2-dichloroethane (DCE) solution at reflux, afforded the related chloride **6**, which was directly treated with **3** in dichloromethane to give rise to expected target product **7**. The related amide **8**, which lacks the NOPD framework, was obtained in an analogous way from **5** and diethylamine hydrochloride.

Spectroscopic and photochemical properties

Figure 1 A shows the absorption spectra of molecular hybrid **7** and, for comparison, those of identical concentrations of model compounds **4** and **8**. The spectrum of **7** is characterized by two distinct absorptions at 420 and 566 nm, which correspond to the NO nitroaniline derivative and the rhodamine moiety. These spectral features reflect the sum of the spectra of **4** and **8** quite well and account for the negligible interaction between the two chromophoric units of conjugate **7** in the ground state.
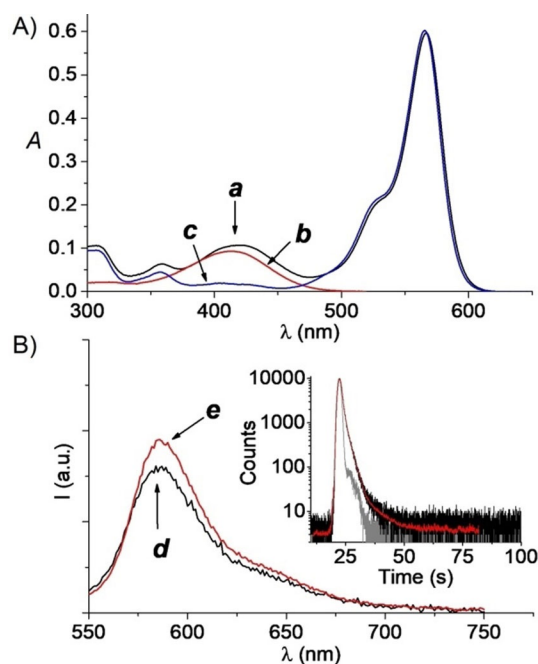

Scheme 1. Synthesis of target compounds **4**, **7** and **8**: a) K₂CO₃, CH₃CN, Δ, 44 %; b) (CH₃CO)₂O, Et₃N, CH₂Cl₂, 63 %; c) POCl₃, DCE, Δ; d) **3**, Et₃N, CH₂Cl₂, 83 %; e) Et₂NH·HCl, Et₃N, CH₂Cl₂, 97 %.

Figure 1. A) Absorption spectra of 6 μM solutions of **7** (*a*), **4** (*b*) and **8** (*c*). B) Fluorescence emission spectra of optically matched solutions of **7** (*d*) and **8** (*e*) recorded at $\lambda_{ex} = 480$ nm. The inset shows the fluorescence decay profiles (black line) and the related fitting (red line) at 590 nm for **7**. The grey lines show the prompt signal. Phosphate buffer (pH 7.4, 10 mM with 10% DMSO); $T = 25\,°C$.

The fluorescence properties of **7** and model compound **8** are shown in Figure 1B. Steady-state emissions reveal the typical profile of the rhodamine fluorophore, in both cases, with identical emission maxima and very similar fluorescence quantum yields ($\Phi_F = 0.45$ and 0.40, respectively), calculated by using rhodamine B in EtOH as standard. The fluorescence decay was, in both cases, tri-exponential with a dominant component of ~1.5 ns (see insets Figure 1B). This multi-exponential behavior suggests that **7** and **8** probably partially self-aggregate in the solvent used, most likely due to the relatively non-polar character of the compounds. This was confirmed by measurements performed in neat ethanol where the values of Φ_F increased to 0.58 and decay was mono-exponential, with a lifetime of 1.8 ns for both **7** and **8**. Overall, the behavior observed accounts for a good preservation of the emissive properties of the rhodamine fluorophore in the molecular hybrid, which is a result of the lack of any significant interaction between the rhodamine and the nitroaniline components in the excited singlet state. This is in accordance with our design, because: 1) quenching by photoinduced energy transfer from the rhodamine to the nitroaniline derivative is thermodynamically not allowed, as the lowest excited singlet state of the former lies more than 0.5 eV below that of the latter (estimated by the end of the absorption spectra); and 2) quenching by photoinduced electron transfer between the same units, although thermodynamically feasible (estimated through the Rehm–Weller equation taking into account the reduction potential of the nitroaniline derivative (~−0.8 eV) of the rhodamine moiety (~+1 eV) and the energy of the lowest excited state of the

rhodamine (~2 eV)) does not occur probably due to the distance between the chromophores, the short lifetime of the rhodamine fluorophore or specific orientation between the donor and the acceptor occurring in the aggregate form, which are not incline to the electron exchange.

The NO photorelease properties of **7** are demonstrated by the direct and real-time monitoring of this transient species via an ultrasensitive NO electrode which directly detects NO at nanomolar concentration sensitivity using an amperometric technique.[23] The results, illustrated in Figure 2, provide evi-
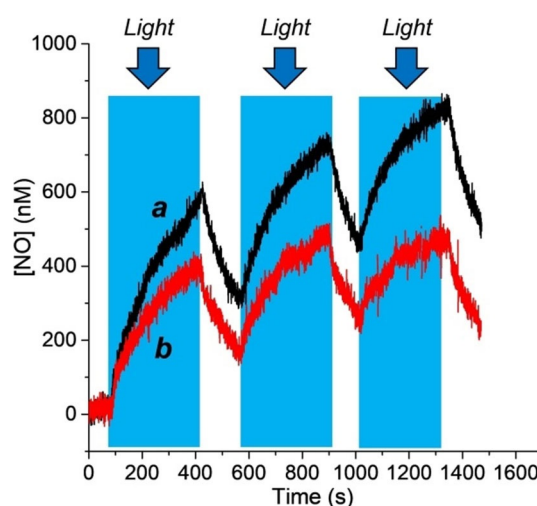

Figure 2. NO release profile observed upon 405 nm light irradiation of 6 μM solutions of **7** (*a*) and the model compound **4** (*b*). Phosphate buffer (pH 7.4, 10 mM with 10% DMSO); $T = 25\,°C$.

dence that the molecular hybrid is stable in the dark, but supplies NO exclusively upon illumination with violet light. Interestingly compound **7** shows a NO release profile slightly improved with respect to **4**. This finding suggests that the rhodamine does not quench the NOPD unit. This is in accordance with the logical assembly of the two components. In fact, although the lowest excited state of rhodamine is 0.5 eV below that of NOPD, potential quenching by photoinduced energy transfer, via the FRET mechanism (through space), from the NOPD to the rhodamine moiety is not allowed due to the lack of NOPD emission (spectral overlap between the emission of the energy donor, that is, NOPD, and the absorption of the energy acceptor, that is, rhodamine, is indispensable if the FRET process is to be feasible).[24] However, the higher NO photorelease efficiency of **7** is somewhat surprising. A tentative explanation for this finding could be an effect of the rhodamine moiety in optimizing the torsional conformation of the nitro group in relation to the aromatic ring and/or stabilizing the phenoxy radical involved into photodecomposition. Another possibility for this enhanced NO photorelease could be a change in the NO photorelease mechanism triggered by a thermodynamically feasible photoinduced electron transfer between the excited nitroaniline chromophore and the rhodamine.

Figure 3 shows the absorption spectral changes observed for a solution of **7** at different irradiation times, under the
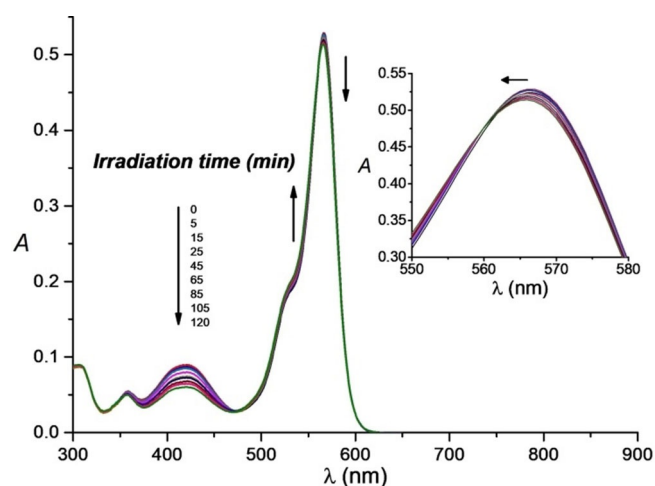
Figure 3. Absorption spectral changes observed for a 6 μM solution of **7** upon 405 nm light irradiation at various time intervals. The inset shows a magnified view of the main absorption spectral region of the rhodamine component of **7**. Phosphate buffer (pH 7.4, 10 mM with 10% DMSO); $T = 25\,^{\circ}C$.

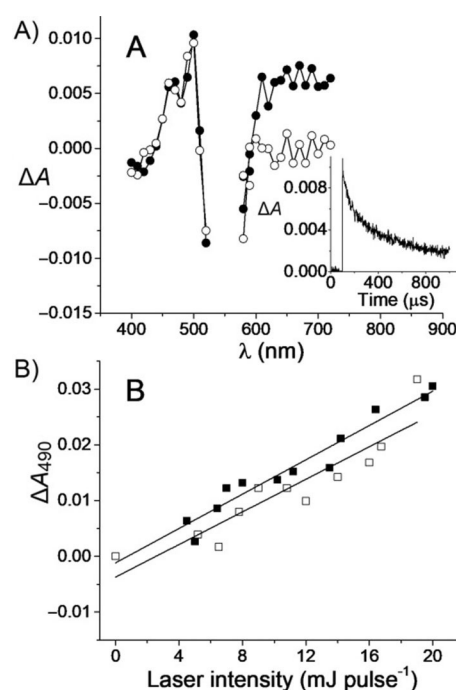**Figure 4.** A) Transient absorption spectra observed 0.3 μs (●) and 3.5 μs (○) after 355 nm laser excitation (6 ns, $E_{532} \approx 10$ mJ/pulse) of a N_2-saturated phosphate buffer solution (pH 7.4, 10 mM) of **7** (6 μM). The inset shows the decay trace monitored at 490 nm. B) Laser intensity dependence of the top ΔA at 490 nm taken 3 μs after the laser pulse for **7** (□) and the model compound **8** (■).

same conditions used for monitoring the NO release. The bleaching of the 420 nm absorption of NOPD is in line with previous observations in similar NOPD units.[14,16–18] However, small but clear spectral changes were also observed around the rhodamine absorption, at 566 nm. As is more easily seen in the zoomed area in the inset of Figure 3, the rhodamine band undergoes a simultaneous hypochromic and blue-shift under violet light irradiation. This spectral behavior has been observed when rhodamine B is irradiated with visible light in the presence of suitable electron acceptors and is due to an *N*-deethylation process, encouraged by the oxidation of the rhodamine moiety to its radical cation.[25]

To gain insight into the transient species formed upon irradiation we performed nanosecond laser flash photolysis experiments. This technique is a powerful tool with which to obtain information on the spectroscopic and kinetic behavior of transient species that absorb in the UV/Vis spectral region. Figure 4A shows the time-resolved spectra of a nitrogen-saturated solution of **7**, recorded at two different delay times together with a 355 nm laser excitation pulse.

The spectrum taken at 0.3 μs shows a maximum at 490 nm, a shoulder at 450 nm and a broad absorption which extends beyond 700 nm. It can be noted that the broad absorption disappears much more rapidly than the 490 nm band which, by contrast, is still present after 3.5 μs. These spectral features are basically the same as those observed in the model compound **8** (data not shown) suggest the occurrence of a photoionization process from the rhodamine moiety. In fact, according to published data,[26] the absorption with a maximum at 490 nm and the shoulder at 450 nm are typical spectral features of the rhodamine B radical cation, whereas the broad absorption, which extends beyond 700 nm, can be assigned to the hydrated electron (e_{aq}).[27] As expected from the high reactivity of e_{aq} with oxygen to form the superoxide anion, $O_2^{\bullet-}$ ($k = 1.75 \times 10^{10}\,M^{-1}\,s^{-1}$),[28] the broad absorption was not present when

the spectrum was recorded at 0.3 μs in a solution of **7** equilibrated with air. According to published work, the decay of the rhodamine radical cation occurred on a long time scale with non-first-order kinetics and was insensitive to the presence of oxygen (inset Figure 4A).[26] To gain insight into the nature of the photoionization process, a laser intensity effect experiment was performed on the absorbance at 490 nm. The results reported in Figure 4B show that the radical cation species has a clearly linear dependence on laser intensity, for **7** and model compound **8**, suggesting that photoionization mainly takes place via a monophotonic process (which also occurs under continuum irradiation with conventional light sources) and with similar efficiency for both compounds. Notably, the laser flash photolysis experiment did not provide evidence for the population of the lowest triplet state of rhodamine, expected to absorb at 410 nm,[26] in **7** or in model compound **8**, which is in good agreement with the well-known inefficiency of population of this excited state in rhodamine B.[26]

Biological studies

NO photorelease in lung adenocarcinoma cells

NO release from **7** and **4** was also studied in cancer cells. NO was detected as nitrite through a Griess assay in human A549 lung adenocarcinoma cells which were either maintained for 30 min in the dark or irradiated for the same time. The results illustrated in Figure 5 show that, as was observed in solution
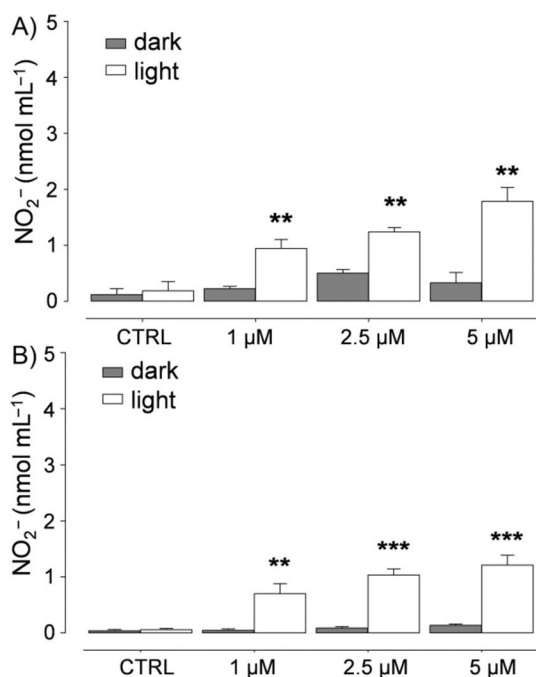
Figure 5. NO photorelease observed in A549 cells incubated with A) **7** and B) model compound **4** and maintained in the dark or irradiated ($\lambda_{ex} = 395$ nm, 7 mW cm^{-2}) for 30 min. Measurements were performed in triplicate, and data are the mean ± SD versus untreated cells (CTRL): **$p < 0.01$; ***$p < 0.001$.

(see Figure 2), no relevant increase in nitrite concentration, with respect to the control, was observed in the dark.

By contrast, irradiation led to the production of nitrite both in hybrid **7** and model compound **4**. Notably, the slight difference observed between the two compounds is similar to direct detection findings of NO in solution (see Figure 2).

Accumulation in mitochondria of human lung adenocarcinoma cells

The remarkable fluorescence of **7** is a very powerful tool to detect its intracellular localization by fluorescence microscopy. To this aim, cells were grown on sterile glass coverslips and transfected with the GFP-E1α pyruvate dehydrogenase expression vector to label mitochondria. After 24 h cells were incubated with 5 μM of compound **7** for 4 h. Samples were rinsed

with PBS, fixed with 4% w/v paraformaldehyde for 15 min, washed three times with PBS and once with water, mounted with 4 μL of Gel Mount Aqueous Mounting analyzed by confocal fluorescence microscopy. As expected in view of the presence of the rhodamine moiety, compound **7** was found to be localized in the mitochondria (Figure 6).

The lack of fluorescence in model compound **4** prompted us to evaluate the capacity of all compounds to accumulate into mitochondria by incubating their 5 μM solutions in A549 cells, according to a previously described procedure.[29] Briefly, the cytosolic and mitochondrial cellular fractions were separated after 4 h of incubation. The amount of each compound in the two fractions was measured by HPLC. The concentration found in the cytosol was 0.86, 1.04, 0.56 μM for **4**, **7**, **8**, respectively; the mitochondrial accumulation was below detection for compound **4**, 0.17 μM for compound **7** and 0.085 μM for 8. The results, expressed as nmol (mg protein)$^{-1}$, are reported in Figure 7. As expected, no accumulation into mitochondria occurred for simple NOPD **4**, which is in contrast with observations for rhodamine-moiety-containing products **7** and **8**.
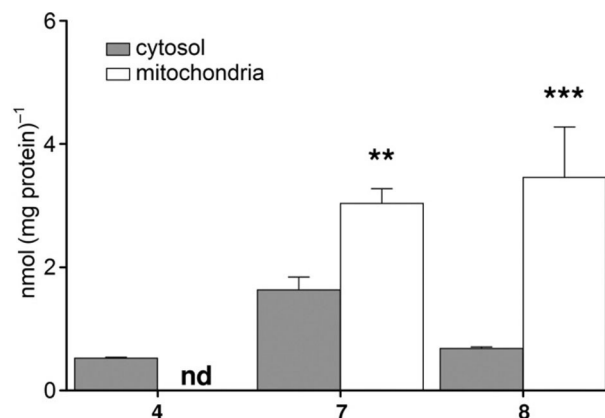
Figure 7. Mitochondrial and cytosolic accumulation of compounds **4**, **7** and **8**. Measurements were performed in triplicate, and data are the mean ± SEM; nd = not detectable; mitochondrial versus cytosolic accumulation: **$p < 0.01$; ***$p < 0.001$.

Cytotoxicity against human lung adenocarcinoma cells

To evaluate the effect of mitochondrial accumulation on cytotoxicity, A549 cells were maintained in Ham's F12 medium
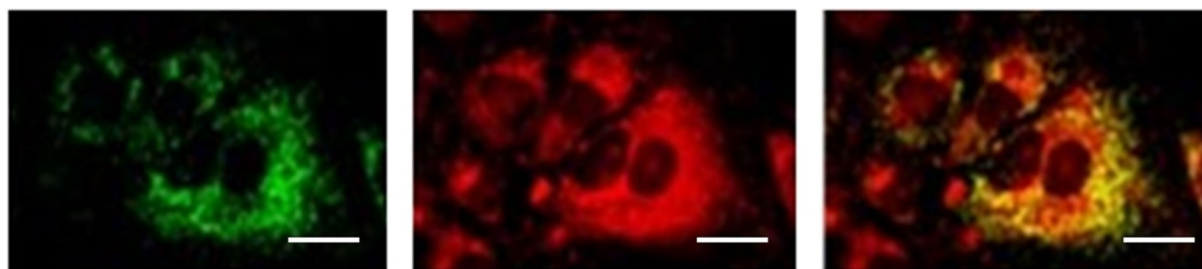

Figure 6. Fluorescence microscopy images of A549 cells incubated for 24 h with the GFP-E1α pyruvate dehydrogenase expression vector to label mitochondria (left) and then treated with compound **7** (center). The merged image is shown at right. Scale bars: 10 μm. Micrographs are representative of three experiments with similar results.

without phenol red and either left for 30 min in the dark, or irradiated in the absence or in the presence of conjugate **7** and model compounds **4** and **8**, at different concentrations. Cytotoxicity was evaluated by the release of lactate dehydrogenase (LDH), a sensitive index for the loss of membrane integrity.[30]

Analysis of the results shows that **4** displays very low toxicity both in the dark and in the light over the whole range of concentrations explored (Figure 8 A). This is in good agreement
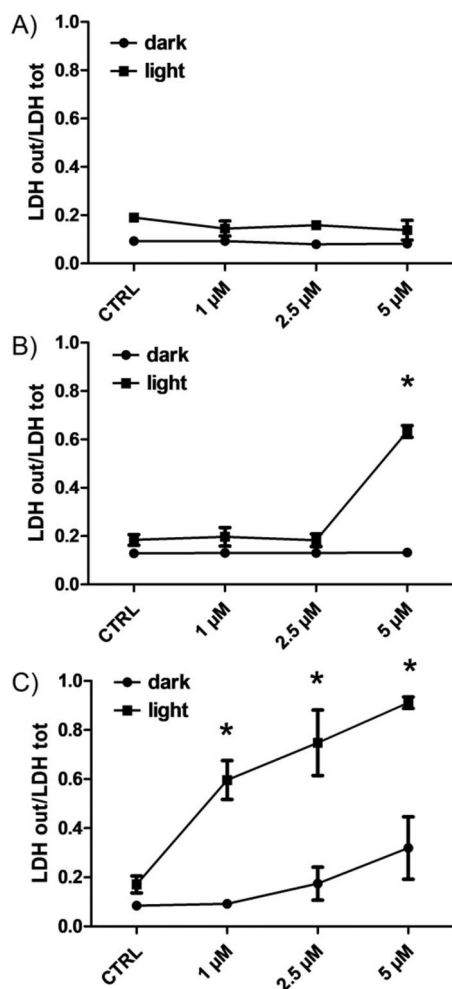

Figure 8. Cytotoxicity of compounds A) **4**, B) **8**, and C) **7** in A549 cells maintained in the dark or irradiated ($\lambda_{ex} = 395$ nm, 7 mW cm^{-2}) for 30 min (light). Measurements were performed in triplicate, and data are mean ± SEM ($n = 3$) versus untreated cells (CTRL): *$p < 0.05$.

with its inability to accumulate into mitochondria. Compound **8** behaves in a slightly different manner (Figure 8 B). In fact, it did not display any relevant toxicity either in the dark or when irradiated at 1 μM and 2.5 μM, but induces toxicity exclusively under irradiation at 5 μM. Such phototoxicity, of course, cannot be attributed to released NO, given that it is not possible from **8**, nor to highly reactive singlet oxygen ($^1O_2$), as no evidence for the formation of the rhodamine triplet state (the key precursor for $^1O_2$ formation)[31] was noted in the time-resolved experiments (see above). Rather, the phototoxicity observed at 5 μM could be due to the formation of other reactive oxygen

species, such as $O_2^{\bullet-}$ (and its decomposition products, that is, H_2O_2). This species can be formed from the photoionization process, similar to what was already proposed for rhodamine 123, which shows monophotonic photoionization and negligible triplet formation.[32]

In contrast to the model compounds, hybrid **7** induces a highly significant cytotoxic effect in a concentration-dependent manner upon irradiation (Figure 8 C). Because this cytotoxicity is not displayed by simple NOPD **4**, in which NO photorelease is similar to that exhibited by **7** in cells (see Figures 2 and 5), this behavior is clearly dependent on the accumulation of the latter into mitochondria. Horinouchi et al. reported a nice study into a rhodamine-NOPD molecular hybrid which induces phototoxicity at 10 μM upon irradiation in a wavelength window that is similar to the one used in our study (below 400 nm).[19b] Although the authors did not use any model compounds, they demonstrated that cell toxicity was directly attributable to photoreleased NO. Interestingly, in our case, phototoxicity was observed at a concentration that was almost one order of magnitude lower. Because no quantitative comparison is possible with these studies, it is hard to discern whether the remarkably high phototoxicity observed in **7** is due to superior NO production, or to a different factor. However, it is important to consider that NO-induced toxicity is usually observed for NO concentrations in the micromolar range.[33] Because, in our case, the lowest concentration that shows phototoxicity was 1 μM and the irradiation time (30 min) was not long enough to induce the complete decomposition of the NO precursor (NO generation < 1 μM), we believe that a mechanism, other than the direct participation of NO as a cytotoxic species, is responsible for the results observed. A plausible hypothesis might be the direct participation of highly reactive peroxynitrite ONOO$^-$ in the observed phototoxicity. This powerful oxidant can, in fact, be effectively generated via the very rapid reaction of NO with the $O_2^{\bullet-}$ ($k = 6.7 \times 10^9$ M^{-1} s^{-1})[34] formed after the photoionization of **7** (see above). Alternatively, formation of superoxide anion by electron-transfer from a photochemically produced radical anion and molecular oxygen can also be considered.

Conclusions

We have demonstrated one of the few examples of molecular systems with the photoregulated release of NO in mitochondria. This has been achieved by the covalent conjugation of a NOPD and a rhodamine targeting unit. The logical design of conjugate **7** allows the properties of the single molecular components to be preserved after conjugation. In fact, comparative studies with suitable model compounds, one lacking the targeting unit and the other the NOPD unit, demonstrated the capability of the molecular hybrid to release NO upon irradiation and to effectively accumulate in the mitochondria of human A549 lung adenocarcinoma cells. Antitumor efficacy was validated against this cancer type, which is hard to eradicate and poorly responsive to conventional chemotherapy, but is suitable for a photodynamic approach to treatment. Only the molecular hybrid triggered toxicity at the very low concen-

tration of 1 μм against these cells following its mitochondrial accumulation and its ability to release NO under light control. Photochemical experiments suggest that, under the action of light, this hybrid can originate $O_2^{-\bullet}$ as well as NO. The fast reaction between these two species may probably lead to the highly reactive $ONOO^-$ which is probably the actual active agent responsible for the phototoxicity observed at the very low concentrations explored. Overall these findings, beyond providing more insight into the photodynamic action of rhodamine-labeled NOPDs, suggest that molecular hybrid **7** is a suitable scaffold for the grafting of appropriate chemotherapeutics and for the development of new multivalent antitumor agents. Projects with this aim are currently in progress in our laboratories.

Experimental Section

Synthesis

All reactions involving air-sensitive reagents were performed under nitrogen in oven-dried glassware using the syringe-septum cap technique. All solvents were purified and degassed before use. Chromatographic separation was carried out under pressure on Merck silica gel 60 using flash-column techniques. Reactions were monitored by thin-layer chromatography (TLC) carried out on 0.25 mm silica gel coated aluminum plates (60 Merck F_{254}) using UV light (254 nm) as the visualizing agent. Unless specified, all reagents were used as received without further purification. Dichloromethane was dried over P_2O_5 and freshly distilled under nitrogen prior to use. Chemical shifts (δ) are given in parts per million (ppm) and the coupling constants (J) in Hertz (Hz). The following abbreviations were used to designate the multiplicities: s = singlet, d = doublet, t = triplet, q = quartet, quint = quintet, m = multiplet, bs = broad singlet. ESI spectra were recorded on a Micromass Quattro API micro (Waters Corporation, Milford, MA, USA) mass spectrometer. Data were processed using a MassLynxSystem (Waters). Purity of final compounds ($\geq$ 95 %) was determined by analytical HPLC analyses on a Merck LiChrospher C_{18} end-capped column (250×4.6 mm ID, 5 μm) using CH_3CN/H_2O or CH_3CN 0.1 % TFA/H_2O 0.1 % TFA as the solvent. HPLC retention times (t_R) were obtained at flow rates of 1.0 mL min^{-1} and the column effluent was monitored using UV as the detector (DAD λ = 226, 254, 400, 560).

N^1,N^3-**diethyl-**N^1**-(4-nitro-3-(trifluoromethyl)phenyl)propane-1,3-diamine (3):** N^1,N^3-diethylpropane-1,3-diamine **1** (18.8 mmol, 2.99 mL) was held at reflux in acetonitrile with 4-chloro-1-nitro-2-(trifluoromethyl)benzene **2** (9.4 mmol, 1.41 mL) in the presence of K_2CO_3 (18.8 mmol, 1.99 g). The reaction mixture was stirred for 72 h and the solvent removed under reduced pressure. The organic phase was diluted with CH_2Cl_2 (20 mL) and washed with water (3× 25 mL), dried over sodium sulfate and concentrated to dryness. The obtained yellow oil was purified by silica gel chromatography using CH_2Cl_2/MeOH (NH$_3$ sat) (97:3 to 90:10 v/v) as eluent to obtain **3** as a yellow solid (R_f = 0.50, 1.319 g, 44 %); mp: 76.6–77.8 °C. ^{1}H NMR (300 MHz, CDCl$_3$): δ = 8.03 (d, J = 9.4 Hz, 1H), 6.98 (d, J = 2.4 Hz, 1H), 6.74 (dd, J = 9.4, 2.8 Hz, 1H), 3.54–3.42 (m, 4H), 2.68 (q, J = 7.1 Hz, 4H), 1.87–1.76 (m, 2H), 1.22 (t, J = 7.1 Hz, 3H), 1.14 ppm (t, J = 7.1 Hz, 3H). ^{13}C NMR (75 MHz, CDCl$_3$): δ = 151.0, 134.7, 129.2, 126.6 (q, $^2J_{CF}$ = 32.5 Hz), 122.5 (q, $^1J_{CF}$ = 273 Hz), 111.9, 109.6 (q, $^3J_{CF}$ = 6.7 Hz), 48.4, 46.5, 45.3, 44.1, 27.5, 14.9, 11.8 ppm. ESI-MS [M+H]$^+$: m/z 320.3. HPLC purity $\geq$ 95 % (acetonitrile TFA

0.1 %/water TFA 0.1 % 40/60 (v/v), flow rate: 1.0 mL min^{-1}, t_R = 9.97 min) at 226, 254 and 400 nm.

N**-ethyl-**N**-(3-(ethyl(4-nitro-3-(trifluoromethyl)phenyl)amino)propyl)acetamide (4):** A solution of **3** (370 mg, 1.16 mmol) in CH_2Cl_2 (10 mL) was stirred for 4 h at 0 °C with acetic anhydride (0.13 mL, 1.4 mmol) and triethylamine (0.15 mL, 1.2 mmol). The reaction mixture was washed with water (3×15 mL) and 1 м HCl (3×15 mL), then dried over sodium sulfate and concentrated to dryness. Purification of the residue by silica gel chromatography using CH_2Cl_2/MeOH (NH$_3$ sat) (99/1 to 97/3 v/v) as the eluent gave the target compound **4** as a yellow oil (R_f = 0.25, 264 mg, 63 %). This compound exists as a mixture of rotamers in a 80:20 ratio as determined by ^{1}H NMR. ^{1}H NMR (300 MHz, CDCl$_3$): δ = 8.06 (d, J = 9.3 Hz, 1H), 6.92–6.85 (m, 1H), 6.72-6-64 (m, 1H), 3.53–3.29 (m, 8H), 2.13 and 2.09 (s, 3H), 1.96–1.80 and 1.84–1.73 (m, 2H), 1.27–1.11 ppm (m, 6H). ^{13}C NMR (75 MHz, CDCl$_3$): δ = 170.7 and 169.8, 150.9 and 150.7, 135.0, 129.4, 126.8 (q, $^2J_{CF}$ = 32.6 Hz), 122.4 (q, $^1J_{CF}$ = 273.2 Hz), 112.0 and 111.9, 109.4 (q, $^3J_{CF}$ = 6.8 Hz), 48.4 and 48.0, 45.7 and 45.5, 45.6 and 43.3, 42.5 and 40.5, 26.7 and 25.8, 21.6 and 21.3, 14.0, 12.9 and 12.0 ppm. ESI-MS [M+Na]$^+$: m/z 384.4. HPLC purity $\geq$ 95 % (acetonitrile/water, 60/40 (v/v), flow rate: 1.0 mL min^{-1}, t_R = 7.00 min) at 226, 254 and 400 nm.

N**-(6-(diethylamino)-9-(2-(ethyl(3-(ethyl(4-nitro-3-(trifluoromethyl)phenyl)amino)propyl)carbamoyl)phenyl)-9,9a-dihydro-3H-xanthen-3-ylidene)-N-ethylethanaminium chloride (7):** A solution of rhodamine B **5** (500 mg, 1.1 mmol) in dichloroethane (5 mL) was held at reflux with POCl$_3$ (0.3 mL, 3.4 mmol) for 4 h. The solvent was removed under reduced pressure to give **6** as a violet foam. This intermediate was dissolved in dry CH_2Cl_2 (15 mL), then NO-photodonor **3** (361 mg, 1.1 mmol) and an excess of triethylamine (0.5 mL) were added and the resulting solution was stirred for 18 h. The reaction mixture was washed with water (3×15 mL), saturated sodium bicarbonate solution (3×15 mL) and 1 м HCl (3× 15 mL), then dried over sodium sulfate and concentrated to dryness. Purification of the residue by silica gel chromatography, using CH_2Cl_2/MeOH (NH$_3$ sat) (98:2 to 90:10 v/v) as the eluent, gave the target compound as a mirrored purple solid (R_f = 0.30, 680 mg, 83 %); mp: 136.0–145.8 °C (this temperature interval indicates the full degradation range time of compound **7**). The ^{1}H and ^{13}C NMR spectra of this compound present two sets of resonances due to restricted rotation around the amide bond at room temperature. This hypothesis was confirmed by a variable-temperature NMR experiment (VT-NMR) performed on compound **7** for which coalescence of the two sets of signals was observed at 60 °C. Compound **7** exists as a mixture of two rotamers in a 70:30 ratio as determined by ^{1}H NMR analysis. ^{1}H NMR (300 MHz, CDCl$_3$, 25 °C): δ = 8.07 and 7.94 (d, J = 9.3 Hz, 1H), 7.67–7.64 and 7.58–7.51 and 7.35–7.32 (m, 4H), 7.41 and 7.22 (d, J = 9.5 Hz, 2H), 7.06–7.01 and 6.96–6.92 (m, 2H), 6.85–6.81 and 6.76–6.71 (m, 2H), 6.61 (d, J = 2.0 Hz, 1H), 6.52 (dd, J = 9.4, 2.5 Hz, 1H), 3.70–3.44 (m, 10H), 3.39–3.08 (m, 8H), 1.33–1.18 (m, 15H), 1.11 and 0.59 ppm (t, J = 7 Hz, 3H). ^{1}H NMR (300 MHz, CDCl$_3$, 60 °C): δ = 7.86 (bs, 1H), 7.68–7.36 (m, 3H), 7.33–7.14 (m, 3H), 7.00–6.60 (m, 6H), 3.60–3.07 (m, 16H), 1.50–0.90 ppm (m, 20H). ^{13}C NMR (75 MHz, CDCl$_3$, 60 °C): δ = 168.4, 157.7, 156.4, 155.9, 150.7, 136.7, 135.4, 132.2, 130.6, 130.1, 129.9, 129.5, 129.0, 126.4 (q, $^2J_{CF}$ = 32.5 Hz), 126.1, 122.5 (q, $^1J_{CF}$ = 273 Hz), 114.5, 113.9, 113.0, 109.8 (q, $^3J_{CF}$ = 6.8 Hz), 96.3, 48.3, 46.1, 45.7, 12.6, 12.0 ppm. ESI-MS [M]$^+$: m/z 744.6. HPLC purity $\geq$ 95 % (acetonitrile TFA 0.1 %/water TFA 0.1 % 90:10 (v/v), flow rate: 1.0 mL min^{-1}, t_R = 7.13 min) at 226, 254, 400 and 560 nm.

N**-(6-(diethylamino)-9-(2-(diethylcarbamoyl)phenyl)-9,9a-dihydro-3H-xanthen-3-ylidene)-N-ethylethanaminium chloride (8):** A

solution of rhodamine B **5** (500 mg, 1.1 mmol) in dichloroethane (5 mL) was held at reflux with $POCl_3$ (0.3 mL, 3.4 mmol) for 4 h. The solvent was removed under reduced pressure to give **6** as violet foam. This intermediate was dissolved in dry CH_2Cl_2 (15 mL), diethylamine hydrochloride (124 mg, 1.1 mmol) and an excess of triethylamine (0.5 mL) were added and the resulting solution was stirred for 18 h. The reaction mixture was washed with water (3× 15 mL), saturated sodium bicarbonate solution (3×15 mL) and 1 M HCl (3×15 mL), then dried over sodium sulfate and concentrated to dryness. The residue was purified by silica gel chromatography using CH_2Cl_2/MeOH (NH_3 sat) (98:2 to 90:10 v/v) as the eluent to give the target compound **8** as a dark-red semi-solid (R_f=0.20, 583 mg, 97%). ^1H NMR (300 MHz, $CDCl_3$) δ=7.67–7.62 (m, 2H), 7.54–7.49 (m, 1H), 7.38–7.31 (m, 1H), 7.24 (d, J=9.4 Hz, 2H), 6.95 (d, J=9.4 Hz, 2H), 6.76 (d, J=1.5 Hz, 2H), 3.67–3.54 (m, 8H), 3.20–3.10 (m, 4H), 1.30 (t, J=7.0 Hz, 12H), 1.08 (t, J=6.8 Hz, 3H), 0.60 ppm (t, J=6.9 Hz, 3H). ^{13}C NMR (75 MHz, $CDCl_3$): δ=167.8, 157.6, 155.8, 155.5, 136.5, 132.1, 130.1, 130.0, 129.9, 126.5, 113.9, 113.7, 96.2, 46.1, 43.4, 38.3, 14.0, 12.5, 11.6 ppm. ESI-MS $[M]^+$: m/z 498.4. HPLC purity $\geq$ 95% (acetonitrile TFA 0.1%/ water TFA 0.1% 90:10 (v/v), flow rate: 1.0 mL min^{-1}, t_R=7.22 min) at 226, 254 and 560 nm.

Instrumentation

^1H NMR and ^{13}C NMR spectra were recorded on a Bruker Avance 300 instrument at 300 and 75 MHz, respectively, and calibrated using $SiMe_4$ as an internal reference. UV/Vis spectra absorption and fluorescence emission spectra were recorded on a JascoV-560 spectrophotometer and a Spex Fluorolog-2 (model F-111) spectrofluorimeter, respectively, in air-equilibrated solutions, using quartz cells with a path length of 1 cm. Fluorescence lifetimes were recorded with the same fluorimeter equipped with a TCSPC Triple Illuminator. The samples were irradiated by a pulsed diode excitation source (Nanoled) at 455 nm. The system allowed measurement of fluorescence lifetimes to be carried out from 200 ps. The multi-exponential fit of the fluorescence decay was obtained using Equation (1):

$$I(t) = \Sigma \alpha_i \exp^{(-t/\tau i)} \qquad (1)$$

Fluorescence quantum yields were determined using optically matched solutions at the excitation wavelength of compounds **7** and **8** and a solution of rhodamine B in EtOH as standard (Φ_f= 0.70)[35] through Equation (2):

$$\Phi_f = \Phi_{f(s)} (In^2/I_{(s)} n^2_{(s)}) \qquad (2)$$

where $\Phi_{f(s)}$ is the fluorescence quantum yield of the standard; I and $I_{(s)}$ are the areas of the fluorescence spectra of compounds and standard, respectively; and n and $n_{(s)}$ are the refraction index of the solvents used for compounds and standard. Absorbance at the excitation wavelength was less than 0.1 in all cases. Absorption spectral changes were monitored by irradiating the sample in a thermostated quartz cell (1 cm path length, 3 mL capacity) under gentle stirring, using a continuum laser with λ_{ex}=405 nm (~100 mW) having a beam diameter of ~1.5 mm.

Amperometric NO detection: NO release for samples in solution was measured with a World Precision Instrument, ISO-NO meter, equipped with a data acquisition system, and based on direct amperometric detection of NO with short response time (< 5 s) and sensitivity range 1 nM −20 μm. The analogue signal was digitalized with a four-channel recording system and transferred to a PC. The

sensor was accurately calibrated by mixing standard solutions of $NaNO_2$ with 0.1 M H_2SO_4 and 0.1 M KI according to the reaction [Eq. (3)]:

$$4H^+ + 2I^- + 2NO_2^- \rightarrow 2H_2O + 2NO + I_2 \qquad (3)$$
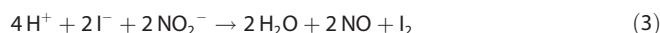
Irradiation was performed in a thermostated quartz cell (1 cm path length, 3 mL capacity) using the continuum laser mentioned above at λ_{ex}=405 nm. NO measurements were carried out under stirring with the electrode positioned outside the light path in order to avoid NO signal artefacts due to photoelectric interference on the ISO-NO electrode.

Laser flash photolysis: All of the samples were excited with the third harmonic of Nd-YAG Continuum Surelite II-10 laser (355 nm, 6 ns FWHM), using quartz cells with a path length of 1.0 cm. The excited solutions were analyzed with a Luzchem Research mLFP-111 apparatus with an orthogonal pump/probe configuration. The probe source was a ceramic xenon lamp coupled to quartz fiber optic cables. The laser pulse and the mLFP-111 system were synchronized by a Tektronix TDS 3032 digitizer, operating in pre-trigger mode. The signals from a compact Hamamatsu photomultiplier were initially captured by the digitizer and then transferred to a personal computer, controlled by Luzchem Research software operating in the National Instruments LabView 5.1 environment. The solutions were deoxygenated via bubbling with a vigorous and constant flux of pure nitrogen (previously saturated with solvent). In all of these experiments, the solutions were renewed after each laser shot (in a flow cell of 1 cm optical path), to prevent photodegradation. The sample temperature was 295±2 K. The energy of the laser pulse was measured at each shot with a SPHD25 Scientech pyroelectric meter.

Biological experiments

Chemicals: Culture media were supplied by Invitrogen Life Technologies (Carlsbad, CA) and plasticware for cell cultures was from Falcon (Becton Dickinson, Franklin Lakes, NJ, USA). The protein content of cell monolayers and lysates was assessed with the BCA kit from Sigma Chemical Co (St. Louis, MO, USA). Unless otherwise specified, all the reagents were from Sigma Chemical Co. Compounds **4**, **7**, **8** were dissolved in dimethyl sulfoxide (DMSO); this stock solution was diluted in culture medium to reach the final concentration. In each experimental condition, the concentration of DMSO in the culture medium was less than 0.1%. Control cells were treated with 0.1% DMSO. Preliminary experiments showed that cells treated with 0.1% DMSO did not differ from cells treated with culture medium without DMSO in any biological assay (data not shown).

Cells: Human lung adenocarcinoma A549 cells, provided by Istituto Zooprofilattico Sperimentale "Bruno Ubertini" (Brescia, Italy), were cultured in Ham's F12 medium supplemented with 10% fetal bovine serum and 1% penicillin–streptomycin. Cell cultures were maintained in a humidified atmosphere at 37 °C and 5% CO_2. When indicated, cells were incubated for 4 h with the compounds and then exposed to the light emitted by a 395 nm, 10 W violet led for 30 min, using an irradiance of 7 mW cm^{-2}, in Ham's F12 medium without phenol red at room temperature. Non-irradiated cells were maintained in a dark room for 30 min in Ham's F12 medium without phenol red at room temperature. After this period, cells were left for 19.5 h in the incubator before the experimental procedures described below.

NO photorelease in cells: After cells were incubated and irradiated as described in the *Cells* section above, 1 mL of cell supernatant was collected, centrifuged for 10 minutes at $13\,000 \times g$ and then the presence of nitrite in the reaction mixture was determined by the Griess assay: 0.5 mL of the reaction mixture was treated with 125 µL of the Griess reagent (4% *w/v* sulfanilamide, 0.2% *w/v* N-naphthylethylenediamine dihydrochloride, 1.47 M phosphoric acid); after 10 min at room temperature, the sample was analyzed by RP-HPLC for detecting the azo dye. HPLC analyses were performed with a HP 1200 chromatograph system (Agilent Technologies, Palo Alto, CA, USA) equipped with a quaternary pump (model G1311A), a membrane degasser (G1322A), a multiple wavelength UV detector (MWD, model G1365D) integrated in the HP1200 system. Data analysis was performed using a HP ChemStation system (Agilent Technologies). The sample was eluted on a HyPURITY Elite C_{18} column (250×4.6 mm, 5 µm, Hypersil, ThermoQuest Corporation, UK). The injection volume was 20 µL (Rheodyne, Cotati, CA, USA). The mobile phase consisting of acetonitrile 0.1% TFA (solvent A) and water 0.1% TFA (solvent B) at a flow rate of 1.0 mL min^{-1} with gradient conditions: 50% A until 4 min, from 50 to 90% A between 4 and 8 min, 90% A between 8 and 12 min, and from 90 to 50% A between 12 and 15 min. The column effluent was monitored at 540 nm referenced against a 800 nm wavelength. Data analysis was performed with Agilent ChemStation. The values obtained from integration of the peak of azo dye were interpolated in a calibration curve obtained using standard solutions of sodium nitrite at 0.5 µM to 50 µM ($r^2 = 0.996$). The yield in nitrite was expressed as percent NO_2^- (mol/mol, relative to the initial compound concentration) ± SEM.

Mitochondria accumulation: 5×10^5 A549 cells were grown on sterile glass coverslips and transfected with the GFP-E1α pyruvate dehydrogenase expression vector (Cell Light BacMan 2.0, Invitrogen Life Technologies) to label mitochondria. After 24 h cells were incubated with 5 µM of compound **7** for 4 h. Samples were rinsed with PBS, fixed with 4% *w/v* paraformaldehyde for 15 min, washed three times with PBS and once with water, mounted with 4 µL of Gel Mount Aqueous Mounting. Slides were analyzed using an Olympus FV300 laser scanning confocal microscope (Olympus Biosystems, Hamburg, Germany; ocular lens: 10×; objective: 60×). For each experimental condition, a minimum of five microscopic fields were examined. For the comparative mitochondrial accumulation experiments, A549 cells were incubated for 4 h with the single compound, then mitochondria were extracted as described earlier.[29] A 50 µL aliquot was sonicated and used for the measurement of protein content or western blotting; the remaining part was stored at $-80\,°C$ until use. To confirm the presence of mitochondrial proteins in the extracts, 10 µg of each sonicated sample was subjected to SDS-PAGE and probed with an anti-VDAC/porin antibody (Abcam; data not shown). The amount of **7** and **8** in the mitochondrial and cytosolic fractions was measured by RP-HPLC with the same instrument and under the same experimental conditions described above. The values obtained from integration of the peak of compounds **7** and **8** were interpolated in calibration curves obtained using standard solutions at 0.05 µM to 5 µM ($r^2 = 0.996$). The amount of **4** in the mitochondrial and cytosolic fractions was measured using a Acquity Ultra Performance LC, Waters Corporation Milford MA, USA, equipped with BSM, SM, CM and PDA detectors. The analytical column was a Zorbax Eclipse XDB-C_{18}, 150×4.6 mm×5 µm. The mobile phase consisted of CH_3CN 0.1% HCOOH/H_2O 0.1% HCOOH 70:30 *v/v*. UPLC retention time (t_R) was obtained at flow rates of 0.5 mL min^{-1} and the column effluent was monitored using Micromass Quattro micro API Esci multi-mode ionization Enabled as the detector. The molecular ion $[M+H]^+$ was

employed for the quantitative measurements of analyte. The MS conditions were as follows: drying gas (nitrogen) heated at $350\,°C$ at a flow rate of 800 L h^{-1}; nebulizer gas (nitrogen) at 80 L h^{-1}; capillary voltage in positive mode at 3000 V; fragmentor voltage at 30 V. The values obtained from integration of the peak of compound **4** were interpolated in calibration curves obtained using standard solutions at 0.1 µM to 5 µM ($r^2 = 0.996$). The amount of compound **4** in the mitochondrial and cytosolic fractions was expressed as nmol (mg protein)$^{-1}$.

Cytotoxicity: The cytotoxic effect of the compounds was measured as the leakage of lactate dehydrogenase (LDH) activity into the extracellular medium with a Synergy HT microplate reader (Bio-Tek Instruments, Winooski, VT, USA), as previously described.[30] Both intracellular and extracellular LDH were measured, then extracellular LDH activity (LDH out) was calculated as a percentage of the total (intracellular + extracellular) LDH activity (LDH tot) in the dish.

Statistical analysis: All data are provided as means ± SEM. The results were analyzed using one-way analysis of variance (ANOVA) and Tukey's test (software: SPSS 21.0 for Windows, SPSS Inc., Chicago, IL, USA); $p < 0.05$ was considered significant.

Acknowledgements

Conflict of interest

The authors declare no conflict of interest.

[1] S. Fulda, L. Galluzzi, G. Kroemer, *Nat. Rev. Drug Discovery* **2010**, *9*, 447.
[2] S. Wen, D. Zhu, D. Huang, *Future Med. Chem.* **2013**, *5*, 53.
[3] G. Chen, F. Wang, D. Trachootham, P. Huang, *Mitochondrion* **2010**, *10*, 614.
[4] S. Demine, N. Reddy, P. Renard, M. Raes, T. Arnould, *Metabolites* **2014**, *3*, 831.
[5] E. Desideri, R. Vegliante, M. R. Ciriolo, *Cancer Lett.* **2015**, *356*, 217.
[6] J. F. Kerwin, J. R. Lancaster, P. L. Feldman, *J. Med. Chem.* **1995**, *38*, 4343.
[7] D. A. Wink, J. R. Mitchell, *Free Radical Biol. Med.* **1998**, *25*, 434.
[8] G. C. Brown, *Front. Biosci.* **2007**, *12*, 1024.
[9] S. Moncada, J. D. Erusalimsky, *Nat. Rev. Mol. Cell Biol.* **2002**, *3*, 214.
[10] S. Goldstein, G. Merényi, *Methods Enzymol.* **2008**, *436*, 49.
[11] a) P. G. Wang, M. Xian, X. Tang, X. Wu, Z. Wen, T. Cai, A. J. Janczuk, *Chem. Rev.* **2002**, *102*, 1091; b) *Nitric Oxide Donors for Pharmaceutical and Biological Applications* (Eds.: P. G. Wang, T. B. Cai, N. Taniguchi), Wiley-VCH, Weinheim, **2005**; c) D. A. Riccio, M. H. Schoenfisch, *Chem. Soc. Rev.* **2012**, *41*, 3731.
[12] S. Huerta, S. Chilka, B. Bonavida, *Int. J. Oncol.* **2008**, *33*, 909.
[13] For example, see: a) S. Sortino, *Chem. Soc. Rev.* **2010**, *39*, 2903; b) P. C. Ford, *Acc. Chem. Res.* **2008**, *41*, 190; c) N. L. Fry, P. K. Mascharak, *Acc. Chem. Res.* **2011**, *44*, 289; d) P. C. Ford, *Nitric Oxide* **2013**, *34*, 56; e) A. Fraix, S. Sortino, *Chem. Asian J.* **2015**, *10*, 1116.
[14] a) E. B. Caruso, S. Petralia, S. Conoci, S. Giuffrida, S. Sortino, *J. Am. Chem. Soc.* **2007**, *129*, 480; b) S. Conoci, S. Petralia, S. Sortino (STMicroelectronics SRL), Eur. Pat. No. EP2051935 A1, US Pat. No. US20090191284, **2006**; c) A. Fraix, N. Marino, S. Sortino, *Top. Curr. Chem.* **2016**, *370*, 225 and references therein.

[15] a) T. Suzuki, O. Nagae, Y. Kato, H. Nakagawa, K. Fukuhara, N. Miyata, *J. Am. Chem. Soc.* **2005**, *127*, 11720; b) K. Kitamura, N. Ieda, K. Hishikawa, T. Suzuki, N. Miyata, K. Fukuhara, H. Nakagawa, *Bioorg. Med. Chem. Lett.* **2014**, *24*, 5660.

[16] A. Fraix, S. Guglielmo, V. Cardile, A. C. E. Graziano, R. Gref, B. Rolando, R. Fruttero, A. Gasco, S. Sortino, *RSC Adv.* **2014**, *4*, 44827.

[17] A. Fraix, M. Blangetti, S. Guglielmo, L. Lazzarato, N. Marino, V. Cardile, A. C. E. Graziano, I. Manet, R. Fruttero, A. Gasco, S. Sortino, *ChemMedChem* **2016**, *11*, 1371.

[18] K. Chegaev, A. Fraix, E. Gazzano, G. E. F. Abd-Ellatef, M. Blangetti, B. Rolando, S. Conoci, C. Riganti, R. Fruttero, A. Gasco, S. Sortino, *ACS Med. Chem. Lett.* **2017**, *8*, 361.

[19] a) T. Horinouchi, H. Nakagawa, T. Suzuki, K. Fukuhara, N. Miyata, *Bioorg. Med. Chem. Lett.* **2011**, *21*, 2000; b) T. Horinouchi, H. Nakagawa, T. Suzuki, K. Fukuhara, N. Miyata, *Chem. Eur. J.* **2011**, *17*, 4809.

[20] a) J. Xu, F. Zeng, H. Wu, S. Wu, *J. Mater. Chem. B* **2015**, *3*, 4904; J. Xu, F. Zeng, H. Wu, S. Wu, *Small* **2014**, *10*, 3750.

[21] a) P. Reungpatthanaphong, S. Dechsupa, J. Meesungnoen, C. Loetchutinat, S. Mankhethorn, *J. Biochem. Biophys. Methods* **2003**, *57*, 1; b) S. Sommerwerk, L. Heller, C. Kerzig, A. E. Kramell, R. Csuk, *Eur. J. Med. Chem.* **2017**, *127*, 1.

[22] S. Swaminathan, J. Garcia-Amoròs, A. Fraix, N. Kandoth, S. Sortino, F. M. Raymo, *Chem. Soc. Rev.* **2014**, *43*, 4167.

[23] P. N. Coneski, M. H. Schoenfisch, *Chem. Soc. Rev.* **2012**, *41*, 3753.

[24] J. R. Lakowicz, *Principles of Fluorescence Spectroscopy, 3rd ed.*, Springer, Amsterdam, **2006**.

[25] X. Hu, T. Mohamood, W. Ma, C. Chen, J. Zhao, *J. Phys. Chem. B* **2006**, *110*, 26012.

[26] P. C. Beaumont, D. G. Johnson, B. J. Parsons, *J. Photochem. Photobiol. A* **1997**, *107*, 175.

[27] G. L. Hug, *Optical Spectra of Non-Metallic Inorganic Transient Species in Aqueous Solution*, National Standards Reference Data Series 69, **1981**, US National Bureau of Standards, Washington, DC.

[28] E. J. Rasburn, *Radiat. Phys. Chem.* **1977**, *10*, 289.

[29] I. Campia, C. Lussiana, G. Pescarmona, D. Ghigo, A. Bosia, C. Riganti, *J. Pharmacol.* **2009**, *158*, 1777.

[30] E. Aldieri, I. Fenoglio, F. Cesano, E. Gazzano, G. Gulino, D. Scarano, A. Attanasio, G. Mazzucco, D. Ghigo, B. Fubini, *J. Toxicol. Environ. Health Part A* **2013**, *76*, 1056.

[31] R. K. Pandey, G. Zheng in *The Porphyrin Handbook, Vol. 6* (Eds.: K. M. Smith, K. Kadish, R. Guilard), Academic Press, San Diego, **2000**. pp. 157–230.

[32] M. W. Ferguson, P. C. Beaumont, S. E. Jones, S. Navaratnam, B. J. Parsons, *Phys. Chem. Chem. Phys.* **1999**, *1*, 261.

[33] a) A. Bishop, J. E. Andderson, *Toxicology* **2005**, *208*, 193; b) A. W. Carpenter, M. H. Schoenfisch, *Chem. Soc. Rev.* **2012**, *41*, 3742.

[34] R. E. Huie, S. Padmaja, *Free Radical Res. Commun.* **1993**, *18*, 195.

[35] M. Montalti, A. Credi, L. Prodi, M. T. Gandolfi, *Handbook of Photochemistry, 3rd ed.*, CRC, Boca Raton, **2006**.